Statistical Characteristics of Free Falling Water Film

A.A Nikoglou, E.P. Hinis, and S.E. Simopoulos
Department of Nuclear Engineering, National Technical University of Athens
Zografos Campus, 9 Heroon Polytechniou, 15780 Athens Greece
anikog@nuclear.ntua.gr; ephinis@mail.ntua.gr; ses@nuclear.ntua.gr

ABSTRACT

Flow of gravitationally falling thin liquid films over the outer cylindrical surfaces with or without concurrent steam flow has always been a fundamental problem of major importance at applied thermal hydraulics, especially, on thermal hydraulic phenomena that occur after a large or small break LOCA such as the rewetting of the overheated fuel elements by a top spraying ECCS and CCFL during reflux condensation. In this study an experimental apparatus has been set up, so as to thoroughly collect liquid films data at low Reynolds numbers by means of needle contact probes. Although this technique is not widely adopted, it is reliable and accurate as other probing techniques and it has the major advantage that it can provide direct measurements of the film characteristics as no calibration is needed. The probes' axial movement is controlled by the use of two step motors capable of 2.5 μm resolution. Step motors are directly connected with a computer that undertakes all the acquisition tasks and thus provides a fully automated measurement procedure. Measurements are performed within the liquid inception region where no surface wave formation is expected and at a proper longitudinal distance from the liquid entrance where the two-wave system would be well developed. Water in ambient pressure is fed to the test section through a slit type distributor with a slit width of 0.25 mm, and then flows freely along the outer surface of a 1.5 m stainless steel cylindrical test section at the temperature of approximately 300 K and volumetric flows between 1 and 3 $L \cdot min^{-1}$. Statistical processing of the collected data, for which probability density distribution of the film thickness, correlation and spectral analysis were used, provides experimental results for the film structure and the film flow characteristics as well. Experimental results for the film thickness distribution, the mean film thickness, the film wave frequency and celerity are presented and further compared to other theoretical and experimental results in the existing literature.

KEYWORDS
Falling films, Probability density, Correlation, Spectral analysis

1. INTRODUCTION

Film flow of viscous liquids presents great practical importance in numerous engineering operations such as distillation, gas absorption, condensation of vapours and other processes where heat and mass transfer are dominant. Many theoretical and experimental studies have been developed on the behaviour of thin liquid films flowing on solid surfaces under the influence of gravity, with or without concurrently flowing gas phase. The first important theoretical work on such liquid film flow was presented by Nusselt [1] for a steady, uniform, two-dimensional flow of a smooth film over an infinitely wide flat plate. This and also other similar early works assume that the liquid surface is free from waves. However, it was substantially documented by Kapitza [2] that all, but the smallest Re numbers, free falling liquid film displays randomly distributed waves on the surface.

Later investigations (e.g. see Rushton et al. [3]), have proven that Nusselt's theoretical approach is not valid at higher flow rates when gravitational and capillary waves are

generated on the free surface. A large number of relevant experiments, summarized in Ambrosini et al. [4], have further shown that at surface locations relatively far from the film inception, the structure of the film surface is random in character and behaves as a two-wave system: large amplitude waves, which carry a significant portion of all the liquid flow, move down the surface with no change in speed or shape and smaller amplitude waves (ripples), which are developed on a substrate film that is formed between the large waves, and which sometimes ride on them. These smaller amplitude waves lose their identity over small distances e.g. see Telles et al. [5], Chu et al, [6] and Ambrosini et al. [4].

The so-far conducted experiments reported in the literature, on the development of free falling films have been carried out in various typical geometries such as: (a) inside or outside a tube e.g see [6-8], (b) on flat plates in various inclinations e.g. [4] and (c) in rectangular channels e.g. see [9, 11], from low to high *Re* numbers, with various liquids. Gas stream was sometimes applied over the liquid film e.g. see [5, 9, 10], in other cases e.g. see [4, 12] heat transfer was established within the liquid film due to heated wall surface.

Various measuring principles have been employed for the measurement of geometrical and kinetic film characteristics namely film thickness distribution, film wave frequency, and mean film velocity; a comprehensive summary of the methods was presented by Hewitt [13]. Conductance probes have been proven to be most suitable for collecting data for films developed on flat plates and in cylindrical or rectangular channels, with or without gas phase flow, whereas needle contact probes seem to be rather appropriate for acquiring data for films developed on outer cylindrical surfaces. The major advantage of the needle contact method over the conductance method is that the formers sensitivity is irrespective of the film thickness, so both extremely thin and extremely thick films can be measured just as accurately. Moreover this technique provides direct measurements as no calibration is needed. In terms of film thickness, the needle contact technique can only provide thickness distribution along the amplitude axis. The film conductance technique, however, may also provide a continuous record of film thickness.

The existing literature on falling film experimental data characteristics, particularly with reference to heat and mass transfer transfer, is rather poor e.g see Sawant et al. [10], Vlachogiannis et al. [14], Bontozoglou et al. [15] and Al-Sibai et al. [16]. To the authors' best knowledge, Takahama et al. [8] presented the last experimental work which investigated falling films using the same data collection principle as that in the present work and that only where film thickness is concerned. Statistical processing of the collected data provides experimental results on the film thickness distribution, film celerity and film wave frequency.

2. EXPERIMENTAL APPARATUS

The main part of the experimental facility is a one-loop water flow experimental rig presented in Hinis et. al [17]. To enable the study of free falling water film characteristics the rig has been interfaced with an additional test section, Nikoglou [18]. This test section consists of a stainless steel circular tube which has been polished and finished accurately reach an outer diameter of 99.96 ± 0.02 mm. The tube is 20 mm thick and 1.5 m long, and it is set up vertically. The tube can be heated by means of three 2 kW, 1 m long electric heating elements accommodated within. Uniform temperature distribution longitudinally and radially is ensured using magnesia powder fill during the assembling. The heating elements are thermostatically controlled and the surface temperature of the tube is monitored by four K-type thermocouples along the tube, which have been embedded at a distance of 1 mm from the outer surface. The 600 L rig heating tank fitted with electric immersion heaters (a total of 36 kW) is used to supply this test section with water of preset temperature in the desired range. The liquid flow rate at the inlet of the test section can be adjusted in the range of 1.0 to 3.5 $L \cdot min^{-1}$ and is measured by a magnetic flow meter. Water is fed to the test section inlet

through a slit type distributor with a slit width of 0.25 mm. Provisions have been made so that the water film flow can be uniform and turbulent free perimetrically on the outer surface of the cylinder in the incept region, even at low Reynolds numbers. Water exits the test section entering a 270 L holding tank and through a centrifugal pump returns back to the heating tank. Fig. 1 presents a schematic of this experimental set-up. Before starting any liquid flow (a) the tube surface has to be thoroughly cleaned with acetone of any superficial slag formations, so as to avoid causing possible dry patch appearance and (b) the rig has to run for an adequate period of time, so as to stabilize water and cylinder temperatures and water inlet flow.

A stand is used for the position of two needle contact probes on a vertical plane containing the cylinder axis. Probe assembling can move along the stand axis and so it can be immobilized at various longitudinal distances from the test section liquid entrance. Experiments have been conducted at longitudinal distances of 40, 80, 160 and 700 mm from the test section liquid entrance. At the region close to the liquid entrance at 40, 80 and 160 mm, even at the highest *Re* number tested, the liquid surface is expected to be free of large waves. On the other hand, the distance of 700 mm makes sure that even at the lowest *Re* number tested in this investigation, the two-wave system would be well developed [8]. Furthermore it is estimated that at this position the maximum *Re* number remains roughly below the critical *Re*, after which fully turbulent flow occurs. Probe spacing has been set at 10 mm, following a compromise between mechanical design and the requirement for non-dispersal of the surface waves between the probes, on the basis of data regarding film wavelength presented by other researchers e.g see [3,5].

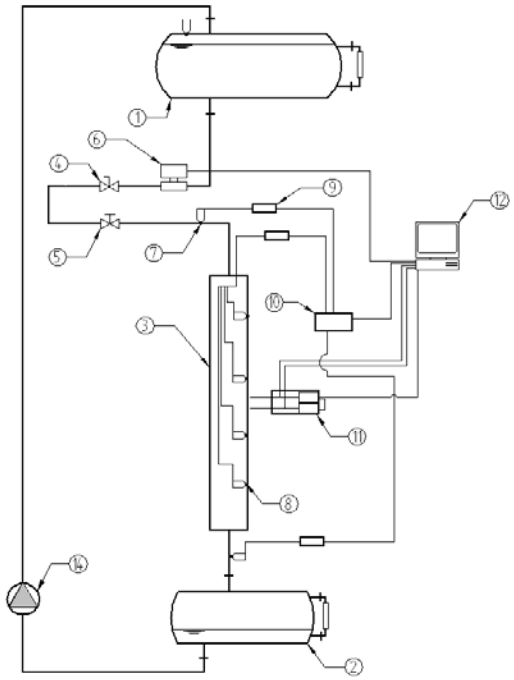

Figure 1. Experimental facility: (1) Heating tank, (2) Holding tank, (3) Test section, (4) Ball valve, (5) Regulating valve, (6) Magnetic flow meter, (7,8) K type Thermocouple, (9) Cold Junction Compensation K type Thermocouple, (10) External multiplexer high gain amplifier, (11) Needle contact assembly, (12) Data acquisition and Needle Probes movement control PC (14) Centrifugal pump.

In the present work, experiments have been conducted at isothermal conditions without heating the test section, which is un-grounded. Electrical signal of 1 kHz frequency and approximately 15 volt amplitude produced by an AC frequency generator is fed to the water film, through the test section distributor. This signal is transmitted to an ADC through the needle probes when conduction exists between the liquid and the probe tip. The data

acquisition setup records the time when probe tips are in contact with the liquid film and the time when probe tips are not, for sequential tip – to - cylinder distances. Tip trace is defined from the zero position of the needle probe, where the needle tip just touches the tube surface to the maximum position where no conduction occurs between probe tip and the liquid for an infinite sample. The radial movement of the probes in and out of the film at 20 μm steps is achieved using computer controlled step motors capable of 2.5 μm resolution. Every measuring device and transducer of the apparatus in on line interfaced with computer, which control its operation status and undertake all data acquisition tasks. In-house developed 80x86 software performs extremely fast and reliable data acquisition at frequency 6.1 kHz. Such a sampling rate results in a Nyquist frequency of approximately 3 kHz eliminating aliasing power spectrum due to folding, since frequencies of that order have never been reported in liquid film waves.

3. FILM THICKNESS MEASUREMENTS

After having a water film stabilized over the test section, one can experimentally determine the probability distribution *P(L)*, by measuring the ratio of the time that a needle tip is in contact with the liquid film to the total measuring time, at a distance *L* from the tube surface. Contact duration data fractions are collected by moving the needle probe tip outwards at 20 μm steps. For each step a data sample of 3 s duration is obtained with sampling frequency of 6.1 kHz. Raw experimental data are smoothed using a *Savitzky–Golay* filter and the smoothed data are in agreement with an *RMS* value in the range of 0.4 to 0.9 %. Fig. 2 presents raw experimental results of probability distribution *P(L)* for *Re* numbers in the range of 230 to 760 and ambient water film temperature at a longitudinal distance of 40 mm from the test section liquid entrance. The resulted film thickness probability distribution sharply decreases from *P(L)=1* to *P(L)=0* within a distance of 20 to 40 μm proving that no surface waves have been developed yet. Fig 3 presents raw and smoothed experimental results of probability distribution *P(L)* at the range 230 to 700 of *Re* number and the same water film temperature at a longitudinal distance of 700 mm from the test section liquid entrance. In this case the resulted film thickness probability distribution sharply decreases reaching a point of inflection and then smoothly fading into *P(L)=0*, forming a long tale; the greater the volumetric flow, the longer the tail. This outcome verifies what has been stated in Takahama et al. [8] and Chu et al. [6] regarding the two-wave system developed in free falling water film considerably far from the liquid entrance section.

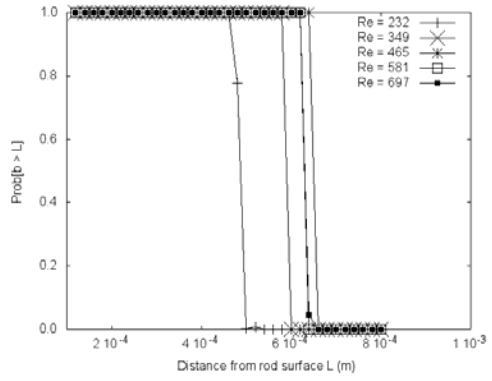

Figure 2. Film Probability distribution at longitudinal distance of 40 mm from liquid entrance

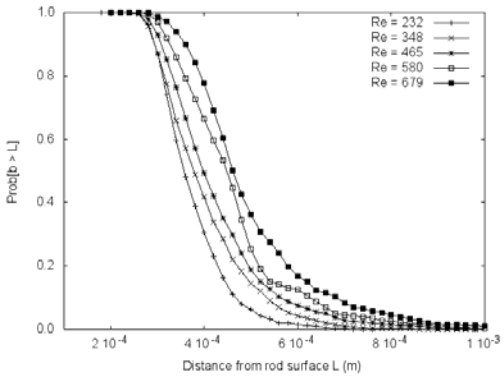

Figure 3. Film thickness probability distribution at longitudinal distance of 700 mm from liquid entrance

It is clearly shown from Figs. 2 and 3 that the liquid film along the flow is always thicker than a minimum value, which stands for the substrate film thickness or equivalently the minimum film thickness δ_{min}. Statistically this value corresponds to the *L* value where *P(L)* is not significantly different from unity. Moreover, it is obvious and it also appears in Figs. 2 and 3

that the liquid film is always thinner than a maximum value, which indicates the maximum film thickness δ_{max}. Statistically, this maximum corresponds to the L value where $P(L)$ is not significantly different from zero. Wave amplitude is expressed as the arithmetic difference between the maximum and the minimum film thickness:

$$\alpha = \delta_{max} - \delta_{min} \tag{1}$$

The area below the film thickness probability curve represents the respective mean film thickness δ_{mean}:

$$\delta_{mean} = \int_0^{\infty} P(L)\, dL \tag{2}$$

Fig. 4 presents experimental data of wave amplitude α, for *Re* number in the range of 230 to 760 at ambient water temperature at longitudinal distances of 40, 80, and 160 mm. It clearly can be seen that by increasing the distance from the liquid entrance, wave amplitude increases; moreover by increasing *Re* number one expands the wave free region. It has been noted in many works that at liquid film formation directly after the distributor the film flows free from surface waves and the waves appear in a short length below the distributor. This length is known as wave inception length. The experimental study of Portalski et al. [19] of wave inception length has stated that for Re number within the region 287 – 2700 the formation of surface waves starts from 7.4 up to 28.8 cm below the distributor. In another experimental investigation, that of Tailby et al. [20] the wave inception length for Re number within the region 70 – 1140 has been found from 4.5 up to 30 cm. In the present work, the wave inception length L_w is experimentally defined via wave amplitude measurement at three positions at the distance of 40, 80 and 160 mm from film distributor along the film flow. The experimental results are summarized as follows Re < 350, L_w < 40 mm, Re < 465 L_w < 80 mm, and Re < 697, L_w < 160 mm. The wave amplitude measurements versus Re number for the three measuring positions are depicted in Fig. 4. In that figure it can be seen that for constant Re number approximately 350 and at distance 40 mm below the liquid entrance the wave amplitude is less than 20μm and the flow is characterized as waveless. Increasing the distance below the liquid entrance to 80 mm and 160 mm the wave amplitude increases and surface waves begin to develop and become visible. So for Re number approximately 350 the wave inception length is estimated at 40 mm. The wave amplitude measurements versus distance from the liquid entrance for different Re numbers are depicted in Fig 5. This conclusion is in concord with the experimental work of Protalski and Tailby.

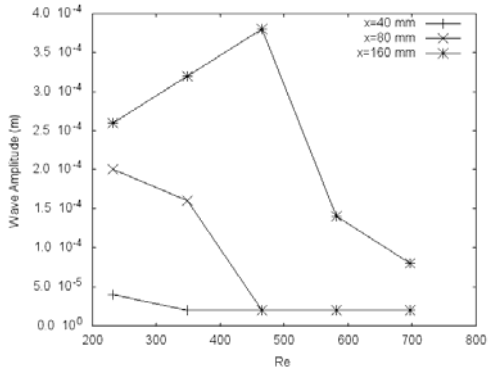

Figure 4. Wave amplitude measurements at distances 40, 80, 160 mm from distributor.

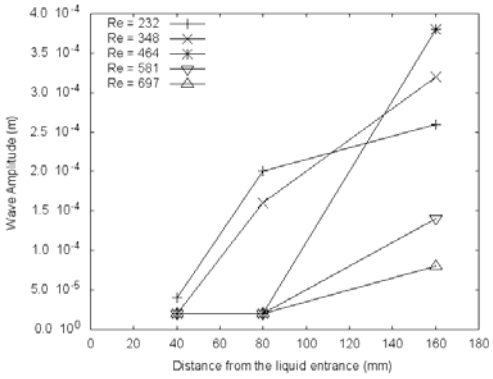

Figure 5. Wave amplitude measurements at various Re numbers

As can be seen from Fig. 2 the shape of the probability distribution shows a significant sensitivity with the *Re* number. At low *Re* numbers the probability distribution shows a rather sharp descent near the minimum film thickness area and a smooth long tail at the maximum film thickness area. As flow-rate increases the first inflection area becomes smoother while the tail of the distribution becomes longer. The derivation of the film probability distribution leads to film thickness density distribution $p(L)= dP(L)/dL$. Film thickness distribution variance s^2 is the second central moment of the density distribution $p(L)$, defined as:

$$s^2 = \int_0^{\infty} (L - \delta_{mean})^2 \, p(L) \, dL \tag{3}$$

The standard deviation σ of film thickness distribution is calculated as the variance square root and gives a measure of the film thickness scattering about its mean value $\delta_{mean.}$ In general, as it can be seen in Fig. 6, standard deviation increases with increasing *Re* number [4, 7].

Minimum, mean and maximum film thickness at the longitudinal position of 700 mm from the liquid film entrance, for the *Re* numbers experimented approximately at 300 K, appears in Fig. 7. It can be seen that the minimum film thickness seems to be almost constant up to 700 *Re* number. Furthermore, the mean film thickness shows a stronger increasing trend with *Re* and finally the maximum film thickness shows an ever sharper increasing trend with *Re.* These results are in agreement with those presented in Karapantsios et al. [7] and Takahama et al. [8]. The film of the former was developed vertically inside a tube of 50 mm inner diameter, while that of the latter was developed outside a tube of 45 mm outer diameter.

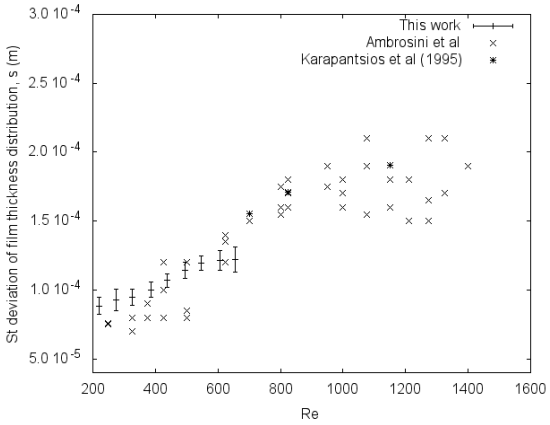

Figure 6. Standard deviation of film thickness distribution vs Re at 301 K.

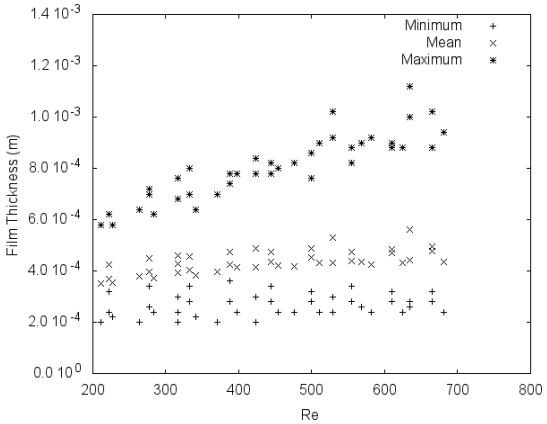

Figure 7. Minimum, mean and maximum film thickness vs Re number

Regarding the increase in minimum film thickness, it should be noted that in Karapantsios et al. 1989 [7] and Takahama et al, [8] the minimum film thickness seems to be almost constant with *Re*; however, this can be attributed to the fact that the wet perimeter in the present experiments is twice as large as the one employed in the aforementioned investigations.
Two additional parameters showing the shape transformation of the probability distribution are the normalized third and fourth central moments (equation 4) of the distribution also known as skewness and kurtosis respectively.

$$\gamma_n = \frac{\mu_n}{\sigma^2} \tag{4}$$

The experimental evaluation of skewness and kurtosis in the present work with *Re* number in the range 200 – 700 can be seen in Figs. 8 and 9. It can be stated that both parameters have a positive correlation with film flow rate as it was expected from the film thickness distribution shape.

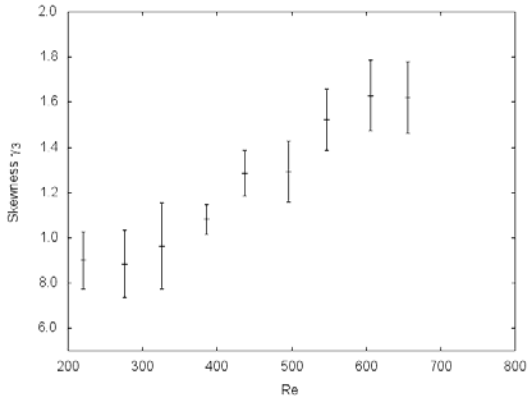

Figure 8. Skewness of the mean film thickness distribution

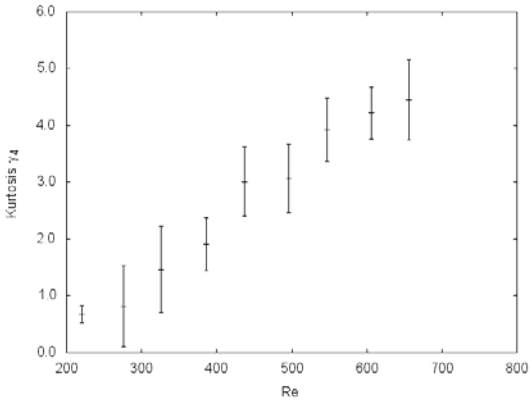

Figure 9. Kurtosis of the mean film thickness distribution

Of great interest is that even though the shape of probability distribution *P(L)* changes with the *Re* number (Fig. 3), where large surface waves have been developed, the value of *P(L)* corresponding to the mean film thickness at various *Re* numbers remains roughly constant about 0.41 ± 0.03 as can be seen in Fig. 10. This has also been reported in [8] with the value of *P(L)* lying between 0.35 and 0.41 for experiments performed at a longitudinal distance of 1700 mm from liquid entrance.

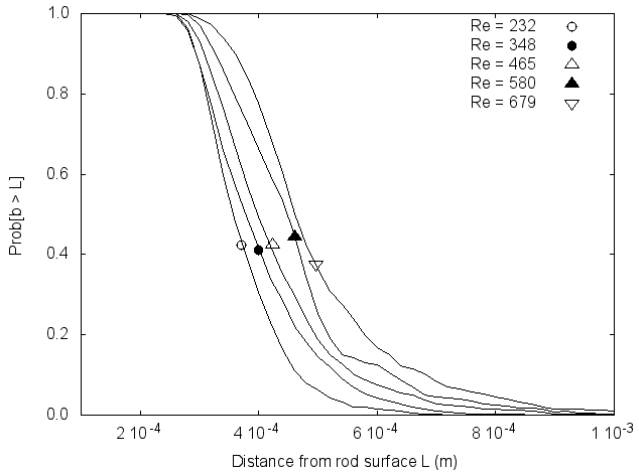

Figure 10. Film thickness probability distribution and mean film thickness at longitudinal distance of 700 mm from liquid entrance

Fig. 11 compares the present experimental results for the mean film thickness with those of three semi-empirical formulae valid for turbulent flow, although in this investigation the flow at ambient temperature can be considered as laminar, and is based on the theoretical standard of Nusselt's theory of laminar flow [1]. The Nusselt formulae can be expressed in the following mathematical form:

$$\delta_{mean} = \alpha \left(\frac{\nu^2}{g}\right)^{1/3} \left(\frac{\Gamma}{\nu}\right)^{b} \tag{5}$$

where: ν is the kinematic viscosity, g is the gravitational force and Γ the volumetric flow rate of liquid per wetted perimeter. The values of a and b are summarized in Table I.

Table I. Semi-empirical formulae factors.

Reference	a	b
Nusselt [1]	$3^{1/3}$	1/3
Takahama et al. [8]	0.473	0.526
Brauer et al. [21]	0.436	8/15
Karapantsios et al. [20]	0.541	0.538
Hajipapas [11] (rms = 2.74%)	2.379	0.269
This Work @ 300 K (rms = 1.80%)	3.712	0.204

The experimental estimations of the mean film thickness of the present work at 300 K are systematically greater than those predicted by the Nusselt theory for laminar flow, as well as those presented in the experimental work of Hajipapas and in the semi-empirical formulae of Brauer, Takahama and Karapantsios. The greatest differences appear in comparison with the semi-empirical formulae and can be attributed to the following reasons. Semi-empirical formulae of Karapantsios and Takahama have been evaluated for *Re* numbers within the regions of 370 – 11020 and ~800 – 8000 respectively, where the flow is fully turbulent. Moreover, the wetted perimeter of the test section in the present experiments is twice as large as that employed in the aforementioned investigations. Additionally, the longitudinal distance of the measurement points from the test section film entrance region is different. In the present work, measurements have been employed at 700 mm from the test section liquid entrance region, while in Karapantsios' work mean film thickness is estimated as the arithmetic mean of six measuring stations at longitudinal distances from 1,720 mm to 2,460 mm from the liquid entrance region and in Takahama' s work the mean film thickness is estimated as the arithmetic mean of eight measurements parametrically the test section and at a distance of 1,700 mm from the liquid entrance region. Hajipapas experimental work shows the least differences in mean film thickness estimations with the present work. This may be due to the fact that Hajipapas experiments have been performed in a cylindrical test section of 100 mm of external diameter and 950 mm of length similar to the one used in the present work. The differences in mean film thickness estimations can be attributed up to a point in the different methology employed for mean film thickness estimations in these two experimental works. In the present work, mean film thickness is estimated as the mean value of the thickness probability distribution, while in Hajipapas it is estimated as the median of the probability distribution.

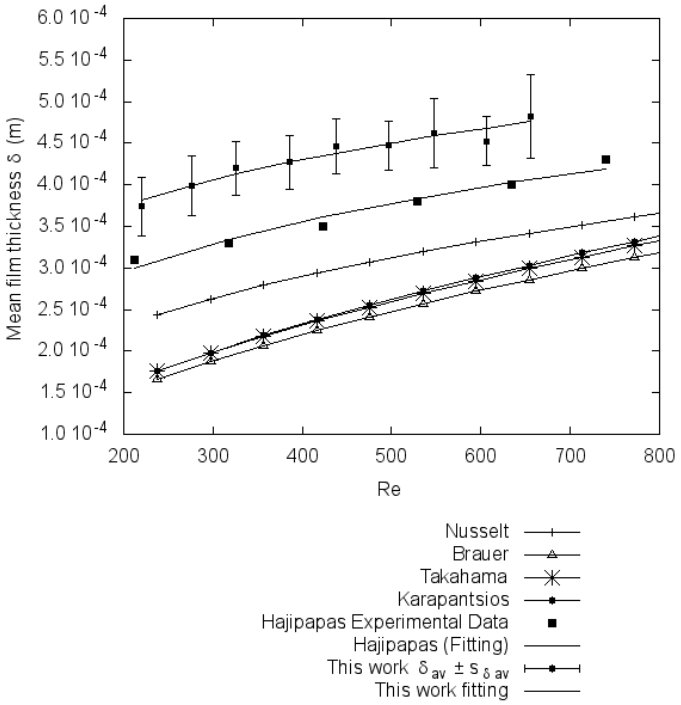

Figure 11. Mean Film Thickness vs Re at 301 K.

4. FILM WAVE FREQUENCY

The accurate definition of the film thickness distribution is essential for the positioning of needle contact probes in order to proceed with further experiments regarding the film wave frequency and the film celerity. Since we are mostly interested in the major bulk waves rather than the small ripples developed it is suggested that the needle tip should be positioned at a surface to tip distance equal to δ_{mean}. The present experimental set-up is capable of precise tip positioning at any position since needle probes can move radially in 2.5 μm steps with the help of computer driven step motors. These steps are far below the minutest observed standard deviation of the measured mean film thickness distribution. Due to the nature of film waves, different thickness measurements at the same point and at the same flow conditions may vary within the standard deviation. Because of that, after having positioned the needle probe at $\delta_{mean} - \sigma$, at the desired longitudinal distance from the test section water entrance and stabilized a water film over the tube outer surface, the acquisition circuitry gathers contact duration data samples moving the probe outwards in 20 μm steps up to needle tip position at $\delta_{mean} + \sigma$ from the tube surface. Each data sample records the time when probe tips are in contact with film water and the time when tips are not for a duration of 8.2 s at a rate of 6,100 samples·s^{-1}. Sweeping the area $\delta_{mean} \pm \sigma$ insures sampling at δ_{mean}. These samples are recognized from the *P(L)* value, which should be approximately 0.41 ± 0.03 as already mentioned.

Treating the film surface fluctuations as an ergodic random function of time, one can employ further stochastic analysis. The autocorrelation function $R_x(\tau)$ of random data describes the general dependence of data values at an instant t on the values at another instant $t + \tau$, and is given by the equation:

$$R_x(\tau) = \lim_{T \to 8.2s} \left(\frac{1}{T}\right) \int_0^T x(t)\, x(t+\tau)\, dt \qquad (6)$$

where *x(t)* in this case is a logical "no" if the tip is not in contact with the film and a logical "yes" if the tip is in contact. The maximum lag time τ_{max} for the autocorrelation function is set

at 0.5 s according to the suggestion of Bendot et. al. [19] and Hajipapas [12]; this corresponds to a bandwidth resolution B_e at the frequency domain, equal to 2.1 Hz, with a normalized standard error ε_r approximately 24%. The autocorrelation function of collected data has been calculated for several different 8.2 s long recordings at the same flow conditions. All obtained autocorrelation functions for every such recording are very similar denoting that ergodicity and periodicity for free falling film waves exists and that an approximately 8 s recording duration at this high sampling rate of 6,100 samples s^{-1} is enough to draw conclusions on the film characteristics at given flow conditions (Bentot and Piersol, 1971). A typical autocorrelation function plot is shown in Fig. 12.

A tool for detecting the dominant film wave frequency *f* possibly masked in the film random background of this experiment is the power spectral density function $G_x(f)$, which specifically for the proven ergodic film data is related to the autocorrelation function by a Fourier transformation and is given by the equation:

$$G_x(f) = 4\int_0^{\tau_{max}} R_x(\tau)\cos(2\pi f\tau)\,d\tau \tag{7}$$

For the purpose of this free falling film analysis, $G_x(f)$ has been calculated for various frequencies, thus allowing to isolate the harmonic with the maximum power spectral density function. A typical power spectral density function plot is presented in Fig. 13.

Out of this analysis it is concluded that the dominant film wave frequency lies in the range of 5 to 11 Hz for *Re* numbers between 250 and 700 as depicted in Fig. 14. However, in some data samples a clear second frequency peak also seems to appear in the range of 10 to 15 Hz as can be seen in Fig. 15 even at low *Re* numbers verifying once again the coexistence of low frequency large waves with smaller waves (ripples) moving over the substrate (Telles and Dukler, [5]), with almost twice the frequency.

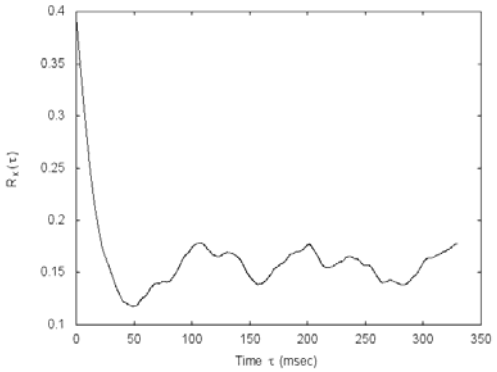

Figure 12. Autocorrelation Function $R_x(\tau\alpha)$ at Re 745

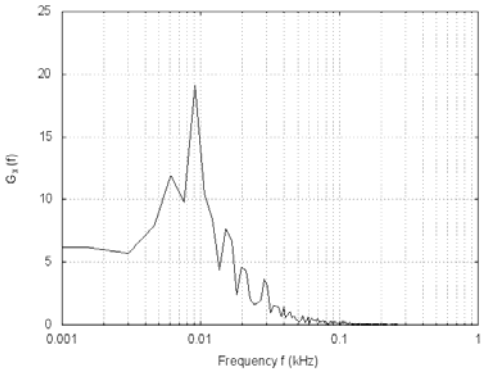

Figure 13. Power Density Function $G_x(f)$ at Re 745

In the experimental work of Hajipapas [12], both the set-up geometry and measuring technique bear strong similarities to those of the present work. The spectral analysis employed in [12] resulted in film wave frequencies in between 9 and 25 Hz for *Re* numbers from 250 to 1,600. Nevertheless, Hajipapas failed to distinguish dominant and secondary frequency peaks, which most probably were masked within the extended frequency range detected.

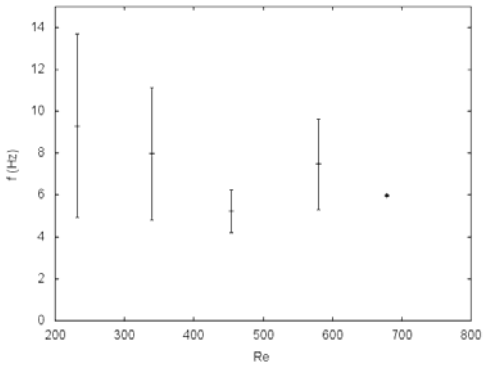

Figure 14. Dominant Film Wave Frequencies vs Re at 301K

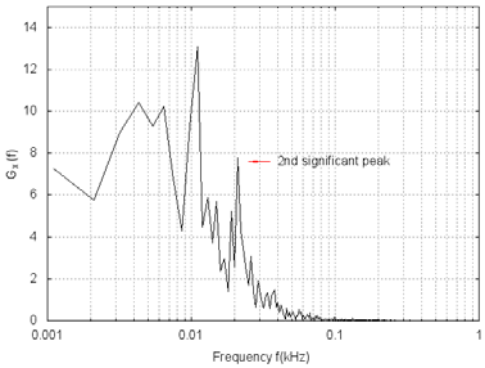

Figure 15. Power Density Function showing the existence of a second significant frequency

The film wave frequency results, which have been reported in the literature [4, 7, 11] at different set-up geometries are generally in agreement with those presented in the present work. However, the existence of a secondary frequency peak range is reported only by Karapantsios et al. [7] for experimental apparatus geometry of an inner tube surface applying parallel-wire conductance probe measuring technique.

5. FILM CELERITY

In case that film celerity estimations are needed, a second needle probe is added 10 mm vertically downstream to the first one at the same tip to surface distance with the upstream probe. Before proceeding to the relevant analysis, it has to be experimentally insured that the penetration effect of the upstream needle tip does not significantly influence the existing free falling film characteristics which are sequentially recorded by the downstream needle probe. To this end three tests have been performed at which both probes interfere with the film flow: (a) calculation of δ_{min}, δ_{mean} and δ_{max} using the downstream probe, (b) autocorrelation analysis and power spectral density using the downstream probe and (c) cross spectral density analysis using both upstream and downstream probes. All tests have been performed for the sampling duration and at the sampling rate already recommended for single probe experiments. Test (a) yielded film thickness distribution estimations systematically lower than the upstream probe but well within the standard deviation calculated for measurements with the upstream probe. Test (b) proved film ergodicity at the downstream needle position at δ_{mean} from the outer tube surface and resulted in the same dominant frequency as calculated from the upstream probe.
For test (c) one has to consider the cross spectral density function $G_{x,y}(f)$ as it may be calculated from both upstream and downstream probes in the manner presented mathematically by the integral:

$$G_{x,y}(f) = \int_0^{\tau_{max}} R_{x,y}(\tau) \exp(i\,2\pi f\tau)\, d\tau \tag{8}$$

where, the cross correlation function $R_{x,y}(\tau)$ is defined as:

$$R_{x,y} = \lim_{T \to 8.2s} \left(\frac{1}{T}\right) \int_0^T x(t)\, y(t+\tau)\, dt \tag{9}$$

and $y(t)$ in this case is a logical “no” if the downstream tip is not in contact with the water film and a logical “yes” if the tip is in contact. Typical cross correlation function for downstream flow and the resulting cross spectral density function are shown in Figs. 16 and 17 respectively.

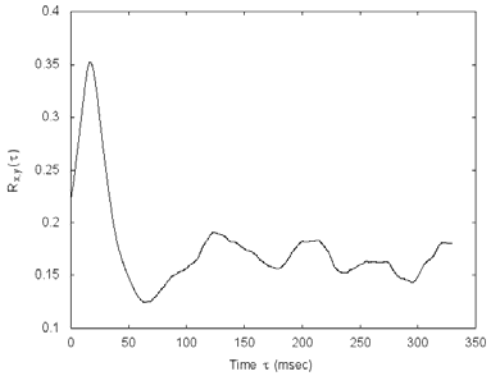

Figure 16. Cross correlation function

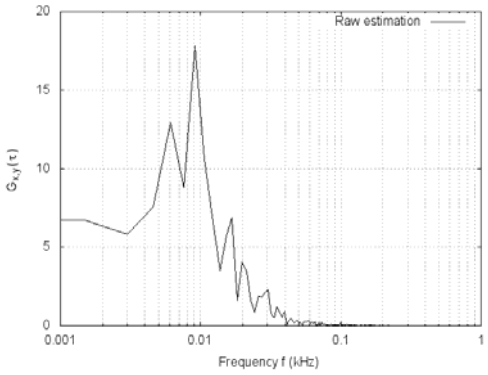

Figure 17. Cross spectral density function.

It has been experimentally verified that application of Eq. (8) on the collected data led again to the same dominant frequency as power spectral density for each probe separately. The autocorrelation and cross-correlation analysis of each data sample, collected with both upstream and downstream probes, should lead to the same value for dominant frequency. Otherwise, each probe records different waves and the data sample is excluded from frequency and celerity calculations. Therefore, tests (a), (b) and(c) have experimentally documented the negligible influence of the two-needle probe system on the free falling film characteristics.

Similar to the frequency calculations for the film celerity estimation both probes are positioned at the estimated mean film thickness. The film celerity *c* is defined as:

$$c = \frac{x}{t_d} \tag{10}$$

where x is the distance between the needle tips (10 mm) and t_d is the time the wave of the dominant frequency needs for covering that distance x.

Cross spectral density function can also be expressed as:

$$G_{x,y}(f) = |G_{x,y}(f)| \exp(-i\theta_{x,y}(f)) \tag{11}$$

Where

$$\theta_{x,y}(f) = t_d \, 2\pi f \tag{12}$$

According to Eq. 12 the phase angle of the cross spectral density and the wave frequency are linearly related provided that waves move between the probe tips without any change of form. As it can be seen from Fig. 18, over the range of dominant frequencies of film wave a linear equation is fitted quite well to experimental data with a coefficient factor R ~ 0.912. This relation proves that the assumption of the non dispersal of the waves between the upstream and downstream probe is fulfilled, and so cross-spectral density can be used for safe estimations of statistically meaningful wave celerity [5].

Applying Eqs (6)-(8) for the experimental results at the dominant film wave frequency, one concludes that the film wave celerity is, as anticipated, a function of *Re* and that in the case of water at ambient temperature at 301 K ranges from 0.5 to 2.5 m s^{-1} for *Re* numbers 250 to 700 (Fig. 19). These results, up to 500 *Re* number, are in agreement both with experiments with the same set-up geometry like Hajipapas, [12] and experiments with different set-up geometries like by Ambrosini et. al. [4] and Drossos et. al. [11].

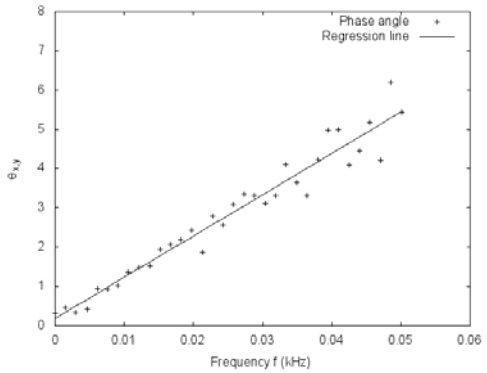

Figure 18. Phase Angle of Cross Spectral Density $G_{x,y}(f)$ at Re 445

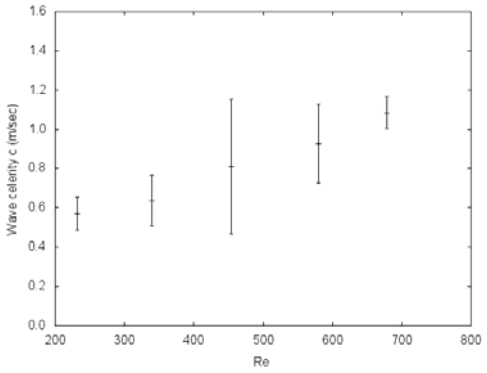

Figure 19. Wave Celerity c vs Re at 301 K

6. CONCLUSIONS

An experimental set-up has been established for the investigation of free falling film characteristics over outer cylindrical surfaces – mainly the film thickness distribution, the film wave frequency and the film celerity. The advantages of this set-up is that it is based on a one -loop water flow experimental rig which is capable of providing water and steam in extremely stable thermodynamic properties using a 600 L reservoir. The measuring technique is based on needle contact probes. This technique, although not widely adopted, has proved to be as reliable, accurate and precise as other probing techniques. It is considered rather successful that with the probes used and the statistical analysis employed a secondary frequency peak range has been detected; such observation and analysis has – to our best knowledge – only been reported once in the literature by Karapantsios et. al. [7]. Additionally, in this particular case of film development on an outer cylindrical surface, needle contact probes constitute the most appropriate technique, since the test cylinder accommodates within its hollow center heating elements for future non-adiabatic film experiments. Therefore, test section construction prohibits the application of e.g. conductance probing techniques. Moreover, needle contact method provides direct measurements of film characteristics since it does not have to be calibrated like e.g. capacitance method.

The results presented in this work provide further data for films developed on the outer surface of a cylindrical wall at low *Re* numbers using the method of needle contact probes for the data acquisition system. These results will be consequently enhanced for non-isothermal flow using the whole range of heating capabilities of the experimental set-up, at even more longitudinal distances from the water entry, aiming to provide a semi-empirical formulae similar to (5) at the aforementioned flow conditions.

7. REFERENCES

1. Nusselt N. 1916., Die Oberflächenkondensation des Wasserdampfes, Zeit. Ver. D. Ing., **vol. 60**, pp. 549-569.
2. Kapitza P.L., "Collected Papers of P.L. Kapitza", Pergamon Ress, **vol. 2**, pp. 662-709, 1962.
3. Rushton E. and G.A.Davies G.A. 1971., "Linear Analysis of Liquid Film Flow", *AIChE Journal*, **vol. 17(3)**, pp. 670-676.
4. Ambrosini W. Forgione N. and Oriolo F. 2002., "Statistical Characteristics of a Water Film Falling down a Flat Plate at Different Inclinations and Temperatures", *International Journal of Multiphase Flow*, **vol. 28**, pp. 1521-1540.
5. Telles A.S and Dukler A.E, "Statistical Characteristics of Thin, Vertical, Wavy, Liquid Films", *Ind. Eng. Chem. Fundam*. **Vol. 9(3)**, pp. 412-421, 1970.

6. Chu K.J. and Dukler A.E. 1974., "Statistical characteristics of Thin, Wavy Films: Part II. Studies of the substrate and its wave structure", *AIChE journal*, **vol. 20(4)**, pp. 695-704.
7. Karapantsios T.D. and Karabelas A.J., "Statistical Characteristics of Free Falling Films at High Reynolds Numbers", *International Journal of Multiphase Flow*, **vol. 15**, pp. 1-21, 1989.
8. Takahama H. and Kato S. 1980., "Longitudinal Flow Characteristics of Vertically Falling Liquid Films without Concurrent Gas Flow", *International Journal of Multiphase Flow*, **vol. 6**, pp 203-215.
9. El-Shanawany M., El-Shirbini, Murgatroyd W. and Bloxham R.D., "A Statistical Analysis of the Behaviour of Waves Formed on the Surface of Thin Film Motivated by Steam", Imperial College of Science and Technology, University of London, 1975.
10. Sawant P., Ishii M., Hazuku T., Takamasa T. and Mori M., "Properties of distubance waves in vertical annular two-phase flow.
11. Drosos E.I.P., Paras S.V. and Karabelas A.J. 2004., "Characteristics of Developing Free Falling Films at intermediate Reynolds and high Kapitza numbers", *International Journal of Mhltiphase Flow*, **vol. 30**, pp. 853-876
12. Hajipapas G.P. 1977., "Surface-Wave Characteristics of Falling Films on a Heated Vertical Column", MSc Thesis, Imperial College of Science and Technology, University of London.
13. Hewitt G.F. 1978., "Measurement of Two-phase Flow Parameters", Academic Press, London.
14. Vlachogiannis M. and Bontazoglou V., "Observations of Solitary Wave Dynamics of Film Flows", *The Journal of Fluid Mechanics*, **vol. 435**, pp. 191-215, 2001.
15. Bontozoglou V. and Papapolymerou G., "Laminar Film Flow Down a Wavy Incline", *International Journal of Multiphase Flow*, **vol. 23(1)**, pp. 69-79, 1997.
16. Al-Sibai F., Leefken A., Renz U., "Local and Instantaneous Distribution of Heat Transfer Rates Through Wavy Films", *International Journal of Thermal Sciences*, **vol. 41**, pp. 658-663, 2002.
17. Hinis E.P. and Simopoulos S.E. 2003., "Experimental investigation of the rewetting process at pressures of 1-7 bar", Kerntechnik, **vol. 68**, pp. 17-22.
18. Nikoglou A.A., "Experimental Investigation of Thin Liquid Films Properties During Free Flow in a Nuclear Power Reactor Channel", PhD Thesis, School of Mechanical Engineering, National Technical University of Athens, 2010.
19. Portalski S and Clegg A. J., "An experimental study of wave inception on falling films", Chemical Engineering Science, **vol 27**, pp 1257 – 1265, 1972.
20. Tailby S. R. and Portalski S. "Wave inception on a liquid film flowing down a hydrodynamically smooth plate", *Chemical Engineering Science*, **vol 17**, pp 283 – 290, 1962.
21. Bendot J.S and Piersol A.G, Random Data: Analysis and Measurement Procedures. Wiley, New York, 1971.
22. Brauer H. Strömung and Wärmeübergang bei Reiselfilmen., VDI-Forschungsheft 457, 1956.
23. Karapantsios T.D. and Karabelas A.J., "Longitudinal Characteristics of Wavy Falling Films", *International Journal of Multiphase Flow*, **vol. 21(1)**, pp. 119-127, 1995.